Post-Periastron ASCA observation of the PSR B1259−63 System

Masaharu HIRAYAMA,[1,2] Fumiaki NAGASE,[1] Marco TAVANI,[3] Victoria M. KASPI,[4] Nobuyuki KAWAI,[5] and Jonathan ARONS[6]

[1] *The Institute of Space and Astronautical Science, 1-1 Yoshinodai 3-chome, Sagamihara, Kanagawa 229*
E-mail(MH) hirayama@astro.isas.ac.jp

[2] *Department of Physics, Faculty of Science, University of Tokyo, 7-3-1 Hongo, Bunkyo-ku, Tokyo 113*

[3] *Columbia Astrophysics Laboratory New York, NY 10027*

[4] *Hubble Fellow, IPAC/Caltech/Jet Propulsion Laboratory Pasadena, CA 91125*

[5] *The Institute of Physical and Chemical Research, 2-1 Hirosawa, Wako, Saitama 351-01*

[6] *Department of Astronomy and Department of Physics, University of California Berkeley, CA 94720*

Submitted to the Publication of the Astronomical Society of Japan

DRAFT: May 8, 1996

Abstract

We report on the results of an *ASCA* observation of the PSR 1259-63 system, containing a 47 ms pulsar in an eccentric 3.4 yr orbit with a Be star, carried out on February 28, 1994. When the pulsar most closely approaches its companion, its pulsed radio emission is eclipsed; the observations reported here were obtained after the radio eclipse ended. The source is clearly detected, and has an X-ray luminosity (1–10 keV) $L_X = (1.03 \pm 0.09) \times 10^{34} (d/2\mathrm{kpc})^2$ erg s^{-1}. The X-ray spectrum is well-represented by a single power law model of photon index, $\alpha = 1.61 \pm 0.06$, and small photoelectric absorption, $N_H = (5.6 \pm 0.6) \times 10^{21}$ cm^{-2}. No significant X-ray pulsations were detected, and an upper limit for the pulsed component is estimated to be 15% of the total X-ray flux, assuming sinusoidal modulation. The characteristics of the X-ray emission detected on February 28, 1994 are similar to those detected by *ASCA* near periastron when the pulsed radio emission from PSR 1259-63 was eclipsed. Our results strongly favor a non-thermal model of X-ray emission driven by synchrotron radiation from relativistic shocked particles in the Pulsar wind interacting with the outflow from the Be star companion.

Key words: pulsars: individual: PSR B1259-63 — stars: neutron — stars: individual: SS2883 — binaries: eclipsing — stars: emission line, Be — x-rays: Stars

1. Introduction

The PSR 111259- 63 pulsar is in a highly eccentric 3.4 yr binary orbit (Johnston et al. 1 992a, b). The pulsar's astrometric, spin, and orbital parameters are determined by radio timing observations (Manchester et al. 1995, hereafter M95). Optical observations identified a 10th mag B2Ve star, SS2883, at a position coincident with the pulsar's position. From its spectral type a mass and a radius of SS2883 is estimated to be $\sim 10\ M_\odot$ and $\sim$ 6-10 $R_\odot$, respectively (Johnston et a]. 1994, hereafter J 94). The distance to the system is somewhat uncertain (J94) and we assume here a compromised distance of 2 kpc.

1 'ulsars 1osc electromagnetic energy by the emission of electromagnetic waves and a MHD wind of relativistic particles. The interaction between the relativistic particle wind and surrounding nebular environments is of particular interest to study modes of high energy emission mediated by relativistic shocks. Typically, the pulsar/nebula interaction is studied in plerionic supernova remnants (e.g., Kennel, Coroniti 1984; Hoshino et al. 1992). However, in principle binary systems containing rapidly rotating pulsars and companion stars with sizeable gaseous outflows can be used for the study of shock interactions. 1 Be stars produce gaseous outflows mostly concentrated in their equatorial planes. The PSR B1259- 63 system containing a rapidly spinning pulsar and a Be star companion is therefore ideal to study the pulsar/outflow interaction (Kochanek 1 993; Tavani, Arons & Kaspi 1 994; Tavani 19W).

Since its discovery, the PSR 111259- 63 system has been observed several times at X-ray energies. *GINGA* (Makino, Aoki, private communication) and *ROSAT* (Cominsky, Roberts, Johnston 1994; Greiner, Tavani, Belloni 1 995) observed the PSR 111259- 63 system near apastron in 1991-1992. A multi-wavelength campaign was organized to observe the January 1994 periastron passage, and the PSR B1259- 63 system was observed three times by *ASCA* (Kaspi et al. 1995; hereafter KTN95) and by the *Compton Gamma-Ray Observatory CGRO* (Tavani et a]. 1995; Grove et al. I 995). The periastron campaign also included radio observations (Johnston et al. 1 995; Manchester et al. 1 995).

A schematic drawing of the pulsar's orbit is shown in Figure 1, in which the pulsar's positions in the orbit at the time of the X-ray observations are shown. *GINGA* failed to detect X-ray emission from the system and gave an upper limit of 2×10^{33} erg s^{-1} (Makino, Aoki, private communication). *ROSAT* detected X-ray emission from the PSR B1259- 63

system with luminosity $L_X \sim 10^{33}$ erg s^{-1} near apastron (Cominsky, Roberts, Johnston 1994; Greiner, Tavani, Belloni 1995). However, due to interstellar absorption and the limited energy band, *ROSAT* results could not constrain the X-ray spectrum. The three *ASCA* observations near periastron (hereafter obs1 on MJD 49349, obs2 on MJD 49362, and obs3 on MJD 49378) allowed the first determination of precise spectral properties of the system. Both the intensity and the spectrum showed an interesting time variable behavior. The main characteristics of the *ASCA* detection of PSR B1259- 63 near periastron are: (1) power-law emission of photon index $\alpha \sim 1.6$ - 1.9; (2) low column density $N_H \sim 6 \times 10^{21}$ cm s^{-1} which remained constant across the periastron region; (3) relatively low X-ray luminosity, $L_X \sim 10^{34}$ erg s^{-1}; (4) lack of pulsed X-ray emission with the pulsar spin period (KTN95). Emission consistent with the power-law interpretation of the *ASCA* results was detected near periastron by the *OSSE* detector on board of *CGRO* up to $\sim$ 200 keV (with luminosity $L_X \sim 10^{34}$ erg s^{-1}, Grove et al. 1995), with a clear indication of a spectral break near 1 10 MeV (Tavani et al. 1995). All the X-ray and gamma-ray observations near periastron were carried out when pulsed radio emission from PSR B1259−63 was not detected, possibly because of free-free absorption or scattering due to intervening gaseous material from the Be star (J95).

The properties (1 4) of the X-ray emission detected by *ASCA* near periastron, as reinforced by the *CGRO* data, strongly favor a non-thermal mode of high-energy emission caused by the interaction of the PSR B1259- 63 relativistic particle pulsar wind with a binary nebular environment. Indeed, the characteristics of all previous X-ray detections are difficult to reconcile with accretion scenarios (Cominsky et al. 1993; KTN95). However, due to the uncertain details of the hydrodynamics and geometry of pulsar/outflow interaction near periastron, the interpretation of X-ray emission in terms of a shock mechanism needs to be confirmed.

We report here on a target-of-opportunity (TOO) observation of the PSR B1259−63 system obtained on February 28, 1994, after the radio pulsar emerged from the periastron eclipse. This new *ASCA* observation therefore provides invaluable information on the mechanism of high-energy emission in a regime where accretion onto the surface of the neutron star, which should quench radio pulsations, is not applicable. We also present a re-analysis of the periastron *ASCA* observations, which confirms previous results (KTN95) and somewhat improves the spectral information.

2. Observation

We observed PSR B1259-63 with the *ASCA* satellite (Tanaka, Inoue, Holt 1994; Serlemitsos et al. 1995) on 1994 February 28 as an *ASCA* '1'()() observation (hereafter 01)s'1). PSR B1259-63 was at true anomaly 127° and radio pulsations became visible after a periastron passage (M95). The net exposure was about 10 ks for each sensor. The two SIS were operated in 1-CCD mode with time resolution of 4 s and the two GIS were in PH mode with time resolution 1.95 ms, high enough in principle to study 48 ms pulsations from PSR B1259-63. The observation is summarized in Table 1.

The X-ray data was reduced with standard sets of analysis tools, including XANADU and FTOOLS packages supplied by ASCA Guest Observer Facility (GOF) at the Goddard Space Flight Center (GSFC) and at the Institute of Space and Astronautical Science (ISAS). In spectral analysis we also used a program "jbldarf" supplied by the ASCA calibration team to calculate an XRT effective area of our observation taking into account of detector's responses. In the temporal analysis we utilized our original programs developed on the ASCA_ANL package, which we have been developing as a platform of flexible analysis of ASCA data. In these programs, however, the GOF-supplied routines were used for temporal corrections, such as a conversion of arrival times of photons to those at solar system barycenter, to keep consistency between results from GOF-supplied tools and 0111"s.

3 ₀ Results

PS1{ 111259-63 was clearly detected with both S1S and GIS, and the X-ray images are consistent with a point source. The position of the X-ray source is coincident with the position of PSR B1259-63 to within 1 arc minute, the accuracy of the attitude determination of ASCA satellite. For the analysis described below, we selected photons within 4 arc minutes from the position of the X-ray source. The SIS0 and SIS1 data were accumulated into a single energy spectrum. The GIS2 and GIS3 data were also summed into another energy spectrum and were combined for the temporal analysis to obtain maximum sensitivity.

As reported in KTN95, an unidentified X-ray source was visible approximately 10' south west of the pulsar in GIS images. We do not discuss this the serendipitous source

in this paper.

3.1. Spectral Analysis

Since the position of PSR B1259- 63 is near the Galactic plane ($b \sim$ - 1°), the Galactic ridge emission gives an important contribution to a background spectrum. The source flux in obs4 was sufficiently weak that the contribution had to be taken into account, although it was negligible for the previous three *ASCA* observations. To estimate the background spectrum near PSR B1259- 63 , we accumulated photons into a spectrum, $S_{\rm BGD}$, from a region which does not include the X-ray point sources in the image. A blank sky spectrum, $B_{\rm BGD}$, was also accumulated in the same region on the detector. Another blank sky spectrum, $B_{\rm SRC}$, was accumulated in the same region as those in which the source spectrum was accumulated. The background behind PSR B1259- 63 is deduced from these spectra by multiplying $S_{\rm BGD}$ with a spectral ratio of the blank sky spectra, $B_{\rm SRC}/B_{\rm BGD}$. We confirmed possible uncertainty in this background spectrum does not affect spectral results described below.

We fit the energy spectra with the GOF-supplied XSPEC software. The results are summarized in Table 2. The spectra of both SIS and GIS are well-represented by a power law model with interstellar absorption. A thermal bremsstrahlung model with interstellar absorption is also acceptable. No emission lines are present. The upper limit for Iron K emission line flux is 3.8×10^{-5} photons cm^{-2} s^{-1} under an assumption of narrow line emission. The absence of emission lines argues in favor of the power law model.

Spectral fits to the SIS and GIS spectra result in the identical spectral parameters within their uncertainties, except for their normalizations. The discrepancy in the SIS and GIS normalizations is consistent with the difference between SIS and GIS fluxes reported by the *ASCA* calibration team (Ishida et al., private communication). In the hope of obtaining more precise spectral parameters, the SIS and GIS spectra were fit simultaneously by a single power law model with a common photon index and a common equivalent column density. Because of the reported discrepancies between SIS and GIS fluxes, the normalizations for the SIS and GIS spectra were treated as independent parameters. Figure 2 shows the result.

We re-analyzed data from obs1, obs2, and obs3in the same way as above; we estimated background spectra including the Galactic ridge emission, and fit the SIS and GIS spectra

simultaneously. In the previous analysis by K TN95, the background spectra did not include the Galactic ridge emission, and Only the SIS data were used for the spectral analysis. The best fit parameters by the re-analysis are listed in Table 3. '1'1)(: parameters are consistent with those from K TN95 within their statisti cal uncertainties.

Confidence contours for a single power law model are plott ed for the four observations in Figure 3. The spectral parameters of obs4 are statistically identical with those of obs3 when the true anomaly was 90°. The equivalent column densities were const ant at a level of $N_{\rm H} \sim 6 \times 10^{21}$ ('111" ^{2} throughout the four observations. Therefore, we conclude the column density is due to interstellar absorption towards PSR B1259−63.

3.2. Temporal Analysis

We first applied a barycentric correction t o the photon arrival times in order to correct for the Doppler effect by orbital motion of the satellite and the motion of the earth around the solar system barycenter. Aft er the conversion, we corrected the arrival times for the 1)oppler shift caused by the motion of 1'S1{ 111259--63 in the binary system. The resultant t ime series data was "epoch-folded" with trial periods near the expected period of PSR B1259- 63, 47.762321 ms, as determined by the radio ephemeris (M95). For each of the folded light curves, we computed

$$S = \sum_{k=1}^{j} \frac{(C_k - C)^2}{\sigma_k^2},$$

where C_k is the observed counting rate of the kth phase bin, C is the averaged counting rate, $\sigma_k = jC/T$, and T is the duration of the observation. The quantity S becomes large if coherent pulsations are in the data.

Figure 4 shows a periodgram, or a plot of the S values versus the trial periods, with $j = 32$. In the figure the data of GIS2 and GIS3 were combined with each other to obtain maximum sensitivity to pulsations. No significant pulsations can be seen in the figure. A folded light curve at the expected period is shown in Figure 5. We also tried Z_n^2 test (Buccheri et al. 1983) for our data. Figure 6 shows a plot of Z_n^2 values against the trial periods for $n = 1, 2, 3, 4$. We have a peak around the expected pulse period in the figure and the peak sightly exceeds a detection limit with 99 % confidence. The absence of pulse detections by the epoch-folding method (Figure 4), together with almost featureless folded light curve (Figure 5), indicates no strong pulsations are in our data, although the

peak in Figure 6 suggests a possible detection of weak X-ray pulsations from the system

Upper limits to the fraction of pulsed photons in our data were estimated with the epoch-folding method discussed by Leahy et al. (1983). The 99% confidence upper limits are listed in Table 4. In addition, time series data were simulated to confirm these upper limits. We confirmed our 99% detection limits by one set of 300 simulated datasets of a constant flux model, and another several sets of 300 time series datasets, each of which includes a sinusoidal profile of 15% to 20% in amplitude. As a result, the 99% upper limit was estimated to lie between 16% and 18%. From these results, we conclude our estimation of the detection limits and the upper limits for pulsations are correct.

The pulsation searches were also performed in two energy bands, 0.5 2 keV and 2 10 keV. Again, no significant pulsations were found. For each set of data the 99% upper limit to the pulsed fractions was also estimated and listed in Table 4 To avoid missing pulse detection due to uncertainty binary parameters, pulsations also searched in P-$\dot{P}$ space as in KTN95. No significant pulsations were detected by the P-$\dot{P}$ search.

4. Discussion and Conclusions

Since the radio pulsar PSR B1259- 63 was visible in February 1994, an accretion-powered mechanism for X-ray emission for the fourth *ASCA* observation seems extremely unlikely. Any reasonable gaseous flow from the Be star towards the pulsar should be strongly perturbed by the pulsar wind pressure. Even for peculiar geometric arrangements between the pulsar wind axis of symmetry and the Be star outflow, a mechanism of accretion onto the neutron star surface which keeps the pulsed fraction very low with a low column density (equal to the periastron value) is difficult to explain. Furthermore, pulsed radio emission produced near the neutron star and propagating in the presence of an accretion flow cannot be reproduced by outflow models that also explain the properties of the emission at periastron (Tavani, Arons 1996 hereafter TA96). We therefore conclude that the X-ray emission in the PSR B1259- 63 system is driven by a mechanism different from accretion. Since the X-ray properties during obs4 are similar to those at periastron (simple power-law emission, low column density, unpulsed emission) is supports the conclusions of KTN95 that the periastron X-ray emission is shock-powered as well.

A number of high-spin-down-luminosity radio pulsars show X-ray pulsations with the spin period (e.g. the Crab, PSR B1509- 58, PSR B1055- 52; see Ogelman (1995) for a

review). Even though most of the emission in the PSR B1259--63 system appears to be dominated by a large "nebular" contribution, pulsar magnetospheric emission may also be present. We found that the upper limit for a pulsed X-ray component in PSR 1112G9- 63 is ~15% of the total flux, corresponding to a pulsed X-ray luminosity $L_{X,pulse} \sim 1.3 \times 10^{33} (d/2\,\mathrm{kpc})^2$ erg s^{-1}, where d is the pulsar distance. If the peak in Figure 6 is a manifestation of pulsed X-ray emission, the pulsed luminosity would be near the allowed upper limit. Magnetospheric X-ray emission is observed to be very stable (e.g., Sekimoto et al. 1995). The pulsed luminosity, as constrained by the *ASCA* obs2 (KTN95), should be less than $4.4 \times 10^{32} (d/2\,\mathrm{kpc})^2$ erg s^{-1}. In addition, *ROSAT* showed the luminosity of the system in 1.0 keV band was less than a few $10^{33} (d/2\,\mathrm{kpc})^2$ erg s^{-1} near apastron and was unpulsed. If the pulsed magnetospheric contribution existed with pulsed luminosity near the upper limit for obs4, the *ROSAT* observations near apastron passage would have detected nearly 100% unpulsed X-rays. In conclusion it is unlikely that the peak in Figure 6 is due to magnetospheric emission.

Shock-powered emission predicts power-law X-ray spectra (TA96). All the 11 *ASCA* observations have revealed that the observed spectra are well-represented by a simple power-law model with a constant interstellar absorption. In the context of the shock-powered model, the emitted spectrum is strongly influenced by synchrotron and inverse Compton cooling of the post-shock particle energy distribution function near periastron. As the pulsar moves away from the periastron region, the shock radius is expected to increase, and both the synchrotron and inverse Compton (IC) cooling have less influence. Based on this scheme, the fact that obs4 shows the hardest spectrum of the four *ASCA* observations is very significant. Since the X-ray spectral slope of the PSR B1259- 63 system at periastron (obs2) was $\alpha 1.96 \pm 0.04$, difference in photon index $\Delta\alpha = 0.35 \pm 0.07$. The X-ray photon index α is a direct reflection of energy index p of electron/positron plasma emitting the X-rays, or $p = 2\alpha - 1$, thus the difference $\Delta\alpha$ corresponds to $\Delta p = 0.7 \pm 0.14$. Since both synchrotron and IC cooling change the energy index by 1.0 when the cooling is fully effective for the plasma, our Δp close to 1.0 indicates that the plasma is sufficiently cooled by the coolings at periastron and relatively free from strong radiative cooling at obs4. The detection of a hard power-law spectrum with $\alpha = 1.6$ in an environment that the radiative cooling is important can therefore constrain the energy index of the post-shock particle distribution function to be less than 2.2.

This research was partially supported by NASA through the grant NAG 5-2730. hill acknowledges support Research Fellowships of the Japan Society for the 1 'romotion of Science for Young Scientists. Part of this research was carried ou t at t he Jet 1 'ropulsion 1 aboratory, California Institute of 'J 'echnology, under contract with the National Aeronautics and Space Administration. V M K ack nowledges support from grant number 111'-1061.01 -94A from the Space Telescope Science Institute, which is operat ed by the Association of Universities for Research in Astronomy, 1 nc., u nder NASA contract NAS5-26555.

Reference

Buccheri, R., Bennett, K.,Bignami, G. F., Caraveo, P. A., Bloemen, J. B. G. M., Hermsen, W., Boriakoff, V., Kanbach, G. et al. 983, A&A 128, 245

Cominsky, L., Roberts, M., Johnston, S. 1994, ApJ 427, 928

Grove, E., Tavani, M., Purcell, W. R., Kurfess, J. D., Strickman, M. S., Arons, J. 995, ApJ 447, L13

Hoshino, M., Arons, J., Gallant, Y.A., Langdon, A.B., 1992, ApJ 390, 454

Johnston, S., Lyne, A. G., Manchester, R. N., Kniffen, D. A., D'Amico, N., Lim, J. Ashworth, M. 1992a, MNRAS 255, 401

Johnston, S., Manchester, R. N., Lyne, A. G., Bailes, M., Kaspi, V. M., Qiao, G., D'A nico, N. 1992b, ApJ 387, L37

Johnston, S., Manchester, R. N., Lyne, A. G., Nicastro, L., Spyromilio, J. 1994, MNRAS 268, 430 (J94)

Johnston, S., Manchester, R. N., Lyne, A. G., D'Amico, N., Gaensler, B. M., Nicastro, L. 1995, MNRAS in press (J95)

Kaspi, V. M., Tavani, M., Nagase, F., Hirayama, M., Hoshino, M., Aoki, T., Kawai, N Arons, J. 1995, ApJ 453, 424 (KTN95)

Kennel C. F., Coroniti F. V. 1984, ApJ 283, 694-709;710-730

Kulkarny, D. A., Darbro, W., Elsner, R. F., Weisskopf, M. C., Kahn, S., Sutherland, P. G., Grindlay, J. E. 1983, ApJ 266, 160

Manchester, R. N., Johnston, S., Lyne, A. G., D'Amico, N., Bailes, M., Nicastro, L. 1995, ApJ, in press

McCollum, B., Castelaz, M. W., Bruhweiler, F. C. 1995, ApJ in preparation

Ögelman H. 1995, *Proceedings of the NATO ASI on the Lives of Neutron Stars*, eds. Alpar, A., Kiziloglu, Ü., van Paradijs, J., Kluwer, Dordrecht

Sekimoto, Y., Hirayama, hi., Kamae, ᵴ., Kawai, N. 1995, ApJ 443, 271

Serlemitsos, P. J., Joalota, 1,., Soong, Y., Kunieda, 1 I., Tawara, Y., Tsusaka, Y., Suzuki, 11., Yamazaki, Y. et al. 1995, PASJ 15, 105

Taylor, J . 1]., Cordes, J. M. 1993, ApJ 411, 6'74

Tanaka, Y., Inoue, 11., Holt, S. S. 1994, PASJ 46, L37

Tavani, M., Arons, .1., Kaspi, V. 1994, ApJ 433, L37

Tavani, M. 1995, in *The Gamma-Ray Sky with COMPTON GRO and SIGMA*, eds. M. Signore, P. Salati, G. Vedrenne (Dordrecht: Kluwer Academics), p. 181.

Tavani, M., Arons, J. 1996, submitted (TA96)

Tavani, M., Grove, J.E., Purcell, W., Hermsen, W., Kuiper, L., Kaaret, 1'., Ford, E., Wilson, R.B., Finger, M., Harmon, B.A., Zhang, S. N., Mattox, J., Thompson, D., Arons, J. 1995, A&A, in press

Table 1: Summary of ASCA TOO observation of PSR B1259- 63

Observation period	1 994 Feb. 28 1 2:00 18:30 (UT)
	49411.50 49411.77 (MJD)
Net exposure (ksec)	7,83 (s1s) / 8.97 (GIS)
Counting rate [a] (cts s^{-1})	0.288,1 0.0005 (S1S) / 0.230:1 0.0004 (GIS)
True Anomaly	127°
Stellar separation [b]	3.9 x 10'3 cm (≈ 550 $R_\odot$)

a) Background-subtracted counting rates not corrected for aspect. Each averaged over SIS0 and SIS1, and GIS2 and GIS3.

b) Estimated for an assumed Be star mass of $M_C \approx 10 M_\odot$.

Table 2: Spectral properties of PSR B1259--63 observed at MJD 49411 (obs4)[a].

	Power law			Thermal bremsstrahlung		
Sensor	Photon index	N_H (10^{21} cm^{-2})	χ^2_ν	kT (keV)	N_H (10^{21} cm^{-2})	χ^2_ν
SIS	1.634 0.09	05.5 ± 0.6	1.15	11^{+5}_{-2}	4.6 ± 0.5	1.25
GIS	1.(M ± 0.10	6.7:1 1.3	0.71	14^{+5}_{-3}	5.0 ± 0.9	0.87

a) Errors are all 90% confidence limits.

Table 3: Spectral parameters for four *ASCA* observations derived from the SIS/GIS simultaneous fits[a].

	Observation (MJD)	Photon index	N_H (10^{21} cm^{-2})	1 10 keV flux [b] SIS	GIS	χ^2_ν
–01)s1	49249	1.78 ± 0.05	"6.() ± ().4	3.434 0.19	2.96:1 0.16	0.97
ol)s2	49362	1.964 0.01	5.8 ± 0.3	1 .54± ().()8	1.'12:1 0.07	0.96
obs3	49378	] .69 ± 0.04	5.8 ± ().'1	3.084 ().18	2.764 ().16	1 .22
01)s'1	'19111	1.61:1 0.06	5.6 ± 0.6	2.154. ().18	1.884 ().16	0.98

a) A II errors are 90 % confidence limits.

b) In units of 10^{-11} erg cm^{-2} s^{-1}.

Table 4: Upper limits[a] to the])111s('(1 component from PSR 111259' 63.

])ataset	0.5 10 keV Fraction[b]	0.5 10 keV Flux[c]	0.5 2 keV Fraction[b]	0.5 2 keV Flux[c]	2 10 keV Fraction[b]	2 10 keV Flux[c]
obs1	8.71	0.0338	15.1	0.020'1	11.8	0.0280"
01)s2	7.58	0.0155	13.4	0.011 4	*10.7*	0.0125
01 s3	8.38	().()3()2	18.4	().()243	*11.3*	0.02?53
ol)s4	15.1	0.0378	22.2	0.0187	*15.3*	0.0249

a) Calculated with 99% confidence.
b) In units of percent.
c) In units of photons s^{-1}.

Figure Captions

Fig. 1. Schematic drawing of the orbit of PSR 1112W 63 . Also shown are the positions of PSR 111259--63 when observed in X-ray band.

Fig. 2. SIS and GIS spectra of PSR B1259- 63 at MJD49411. The spectra are fit simultaneously with a single power law model. Detector responses are folded on the spectral model.

Fig. 3. Confidence contour plots of spectral parameters for a single power law model at MJD 49349(obs1), 49362(obs2), 49378 (obs3), and 49411(obs4).

Fig. 4. A periodgram, i.e., a plot of S values versus trial periods, $P_{\rm trial}$, subtracted by the pulse period, $P_{\rm exp}$ = 47.762321 ms, expected from the radio ephemeris by Manchester et al. (1995) GIS2 and GIS3 data were combined each other. Detection limits for pulsed component are shown in the figure with confidence levels of 90% and 99% under an asumption of a sinusoidal pulse profile.

Fig. 5. Folded light curve at the expected pulse period, $P_{\rm exp}$ = 47.762321 ms, estimated using the radio ephemeris by Manchester et al. (1995). GIS2 and GIS3 data were combined each other.

Fig. 6. Result of Z_n^2 test, i.e., Z_n^2 values for n = 1, 2, 3, 4 versus trial periods, $P_{\rm trial}$, subtracted by the pulse period, $P_{\rm exp}$ = 47.762321 ms, expected from the radio ephemeris by Manchester et al. (1995) GIS2 and GIS3 data were combined each other.

Fig. 7. Flux history of PSR 111259- 63 at MJD 49349(obs1), 49362(obs2), 49378 (obs3), and 49111 (obs4). In the figure results from previous X-ray missions (Makino, Aoki, private communication; Cominsky, Roberts, Johnston 1994; Greiner, Tavani, Belloni 199L) are also plotted after converted to 1 10 keV flux, assuming the best fit parameters in the literatures.

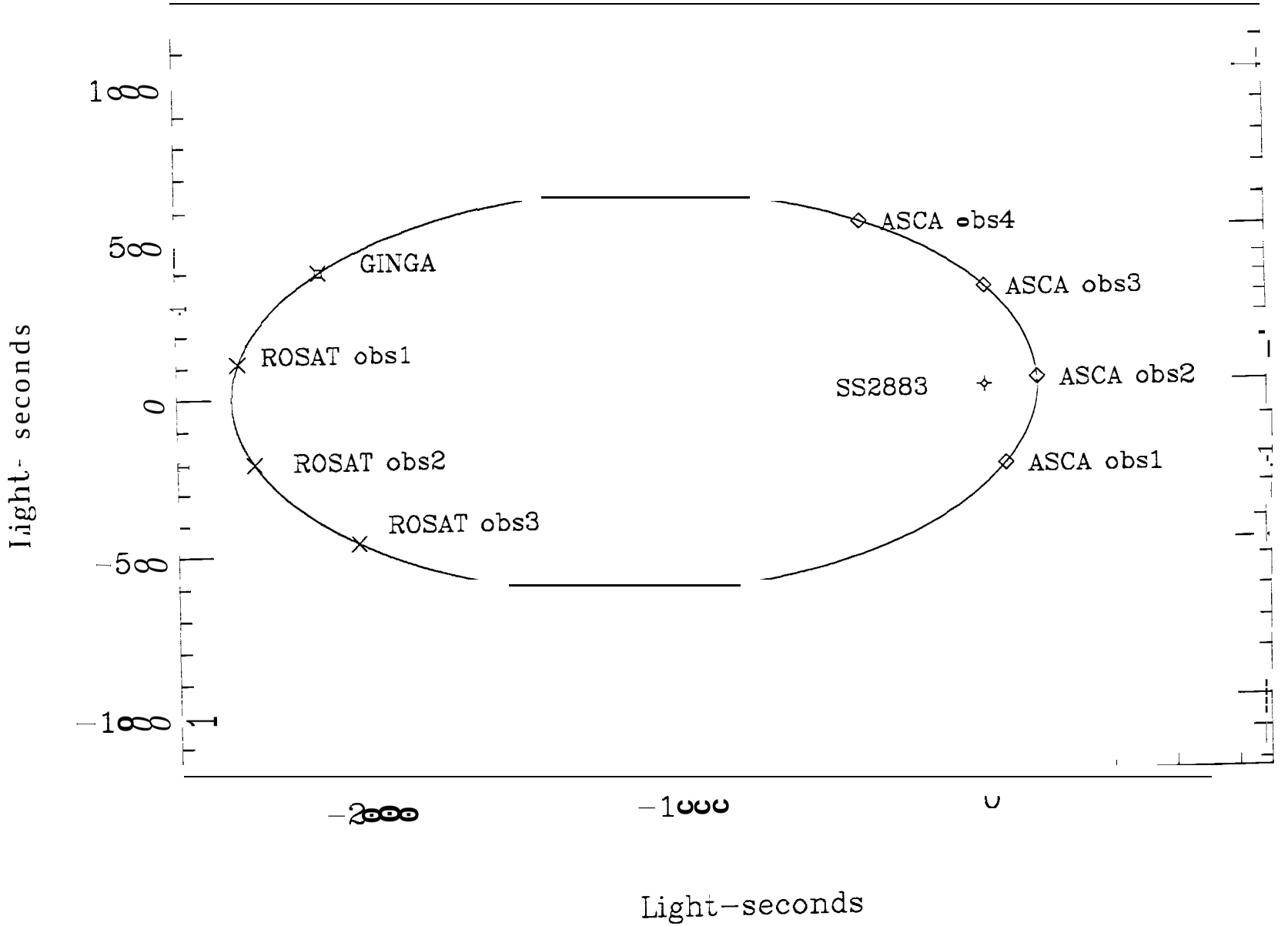
GINGA
ROSAT obs1
ROSAT obs2
ROSAT obs3
ASCA obs4
ASCA obs3
ASCA obs2
ASCA obs1
SS2883
Light- seconds
Light-seconds

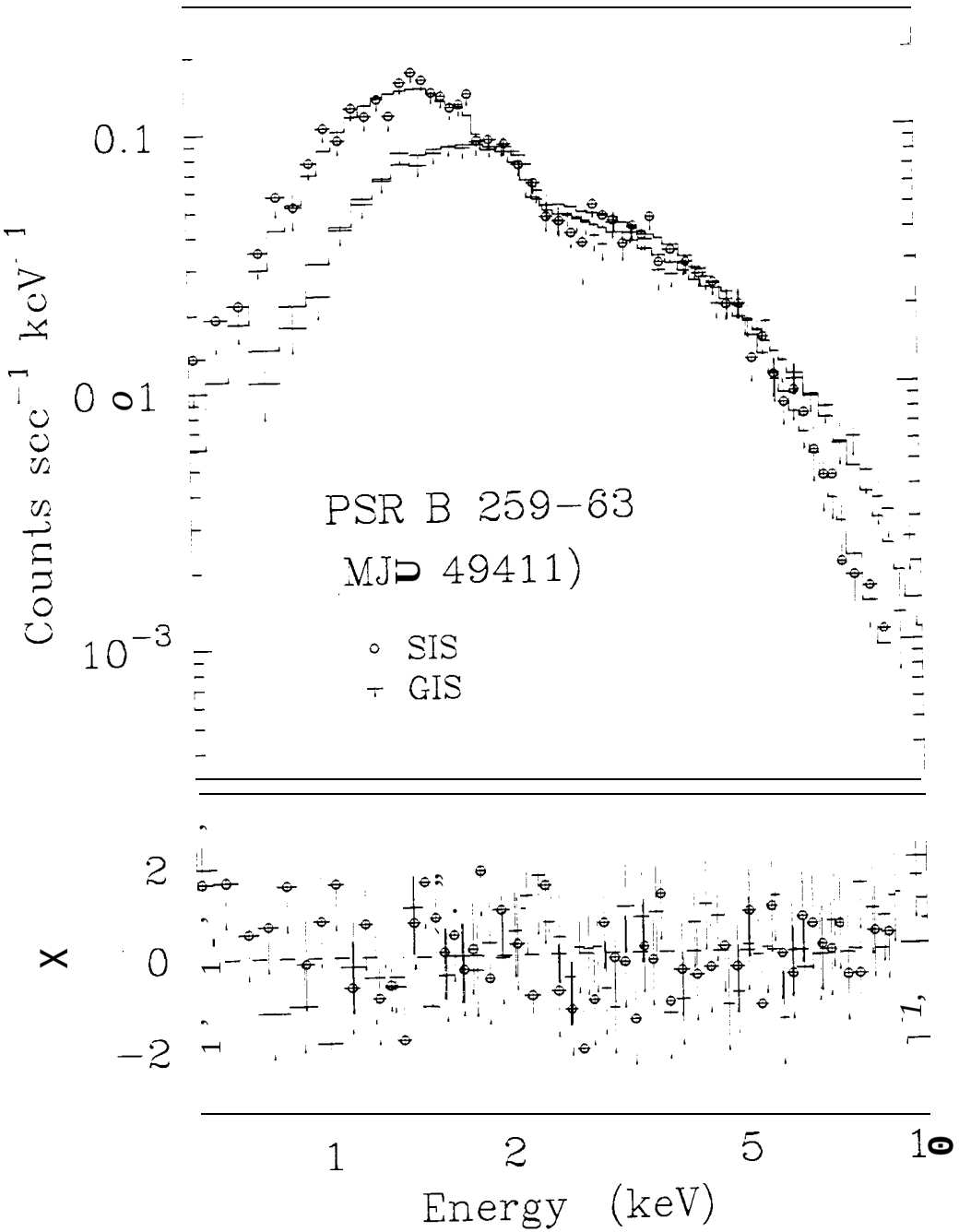
Counts sec^{-1} keV^{-1}
0.1
10^{-3}
PSR B 259−63
MJD 49411)
SIS
GIS
χ
2
0
−2
1
2
5
10
Energy (keV)

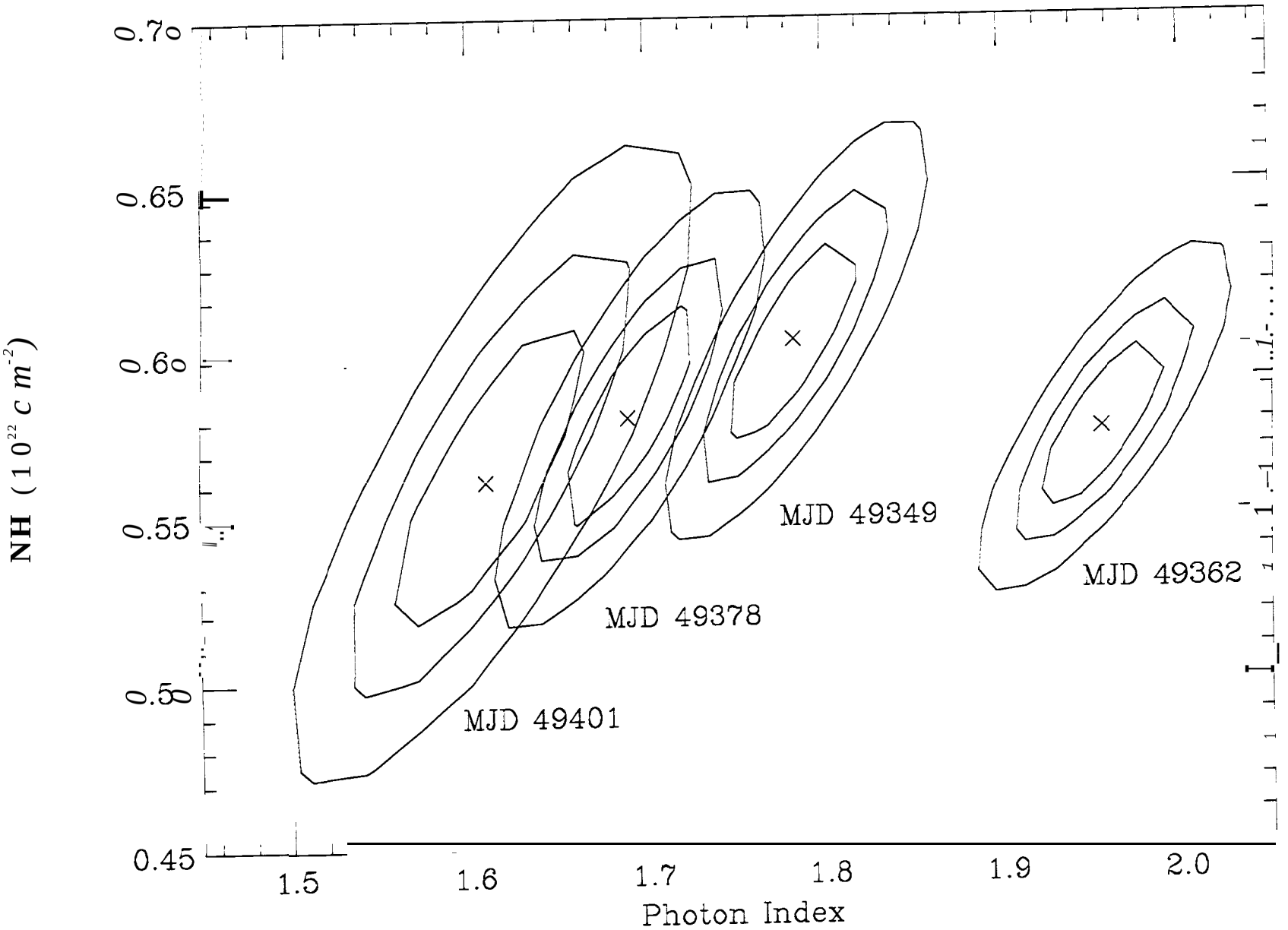
0.7
0.65
0.6
0.55
0.5
0.45
NH (10^{22} c m^{-2})
1.5
1.6
1.7
1.8
1.9
2.0
Photon Index
MJD 49401
MJD 49378
MJD 49349
MJD 49362

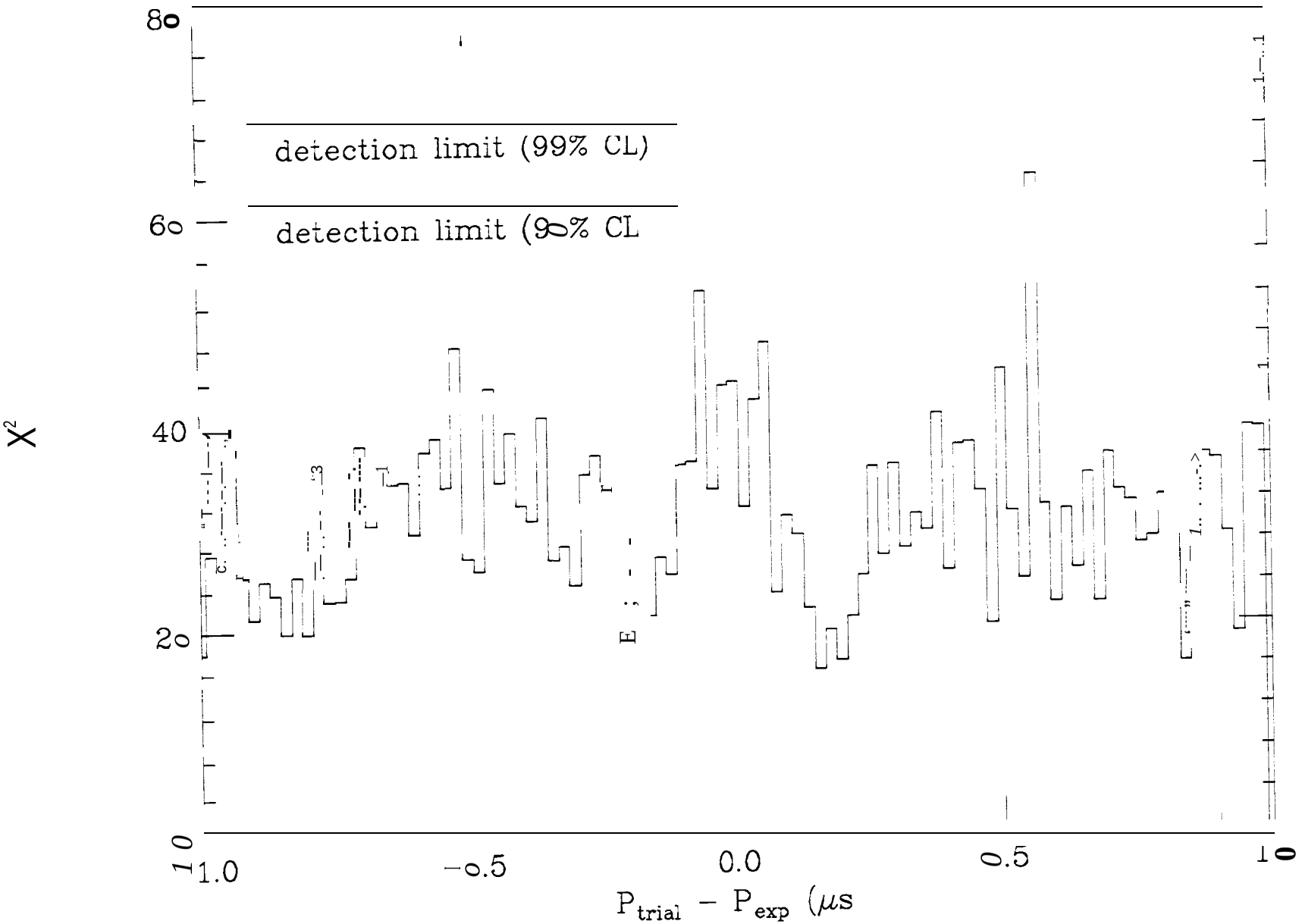
80
60
40
20
0
detection limit (99% CL)
detection limit (95% CL
χ^2
1.0
−0.5
0.0
0.5
1.0
$P_{trial} - P_{exp}$ (μs

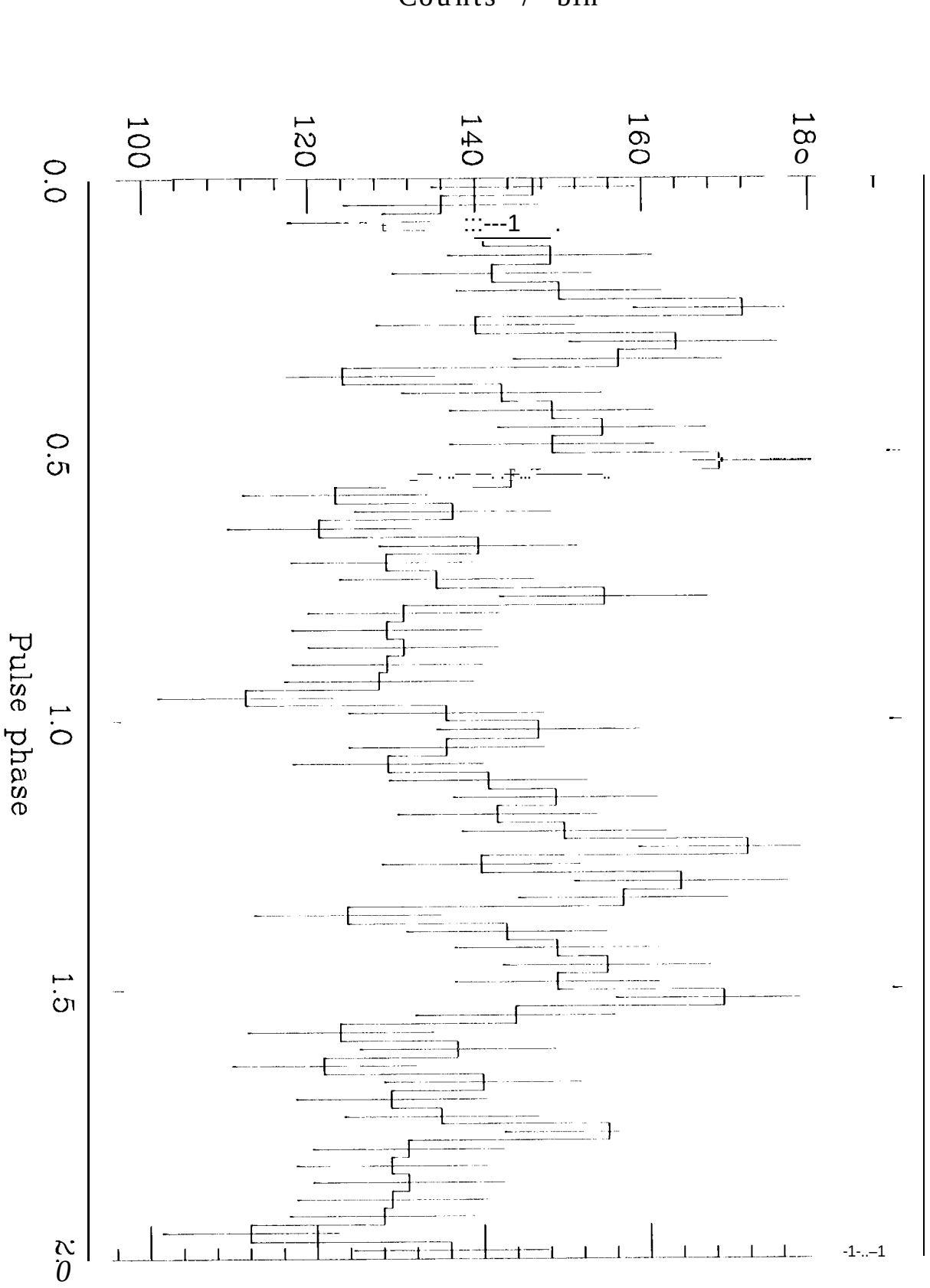
Counts / bin
100
120
140
160
180
0.0
0.5
1.0
1.5
2.0
Pulse phase

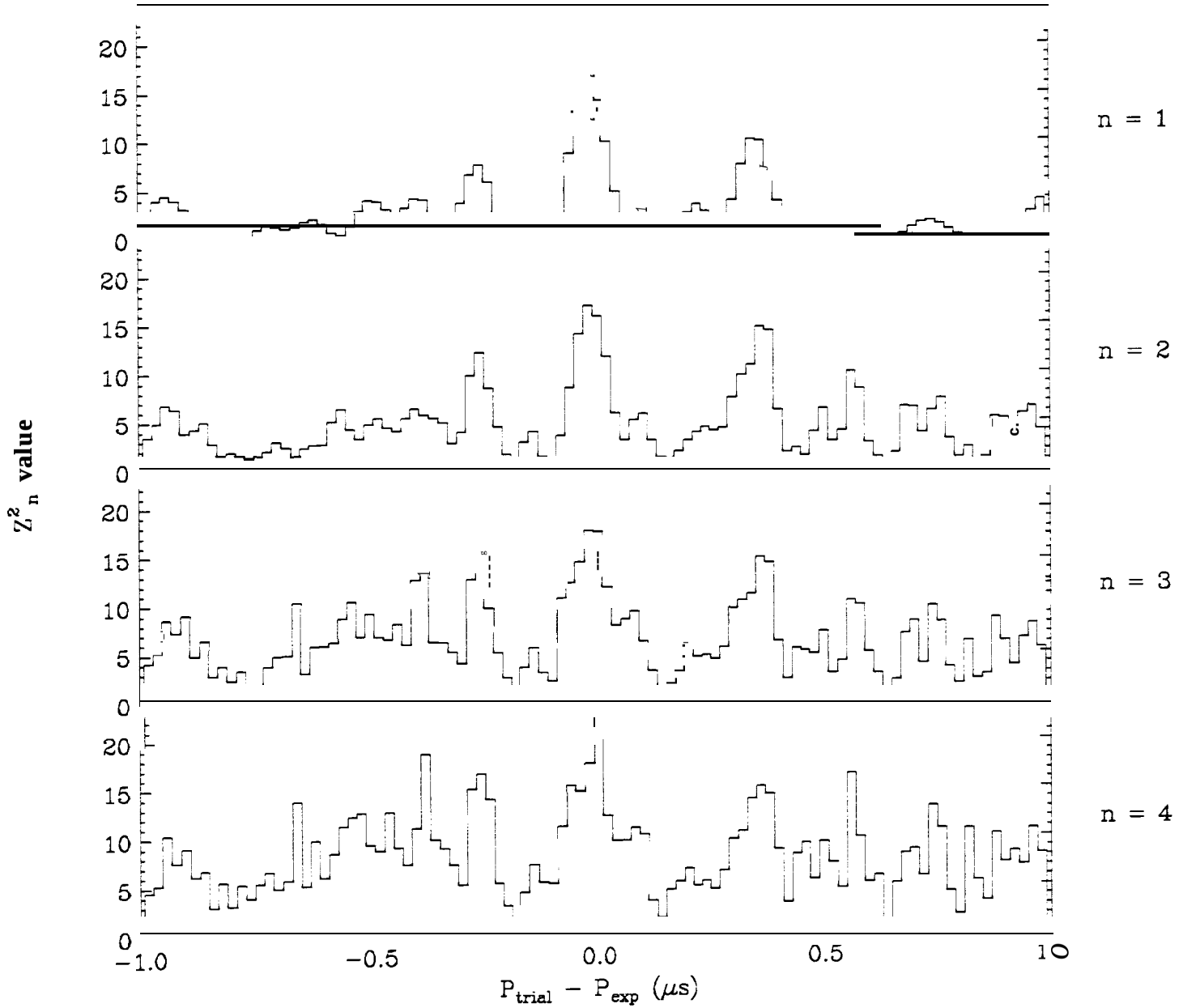
Z^2_n value
n = 1
n = 2
n = 3
n = 4
20
15
10
5
0
−1.0
−0.5
0.0
0.5
1.0
$P_{trial} - P_{exp}$ (μs)

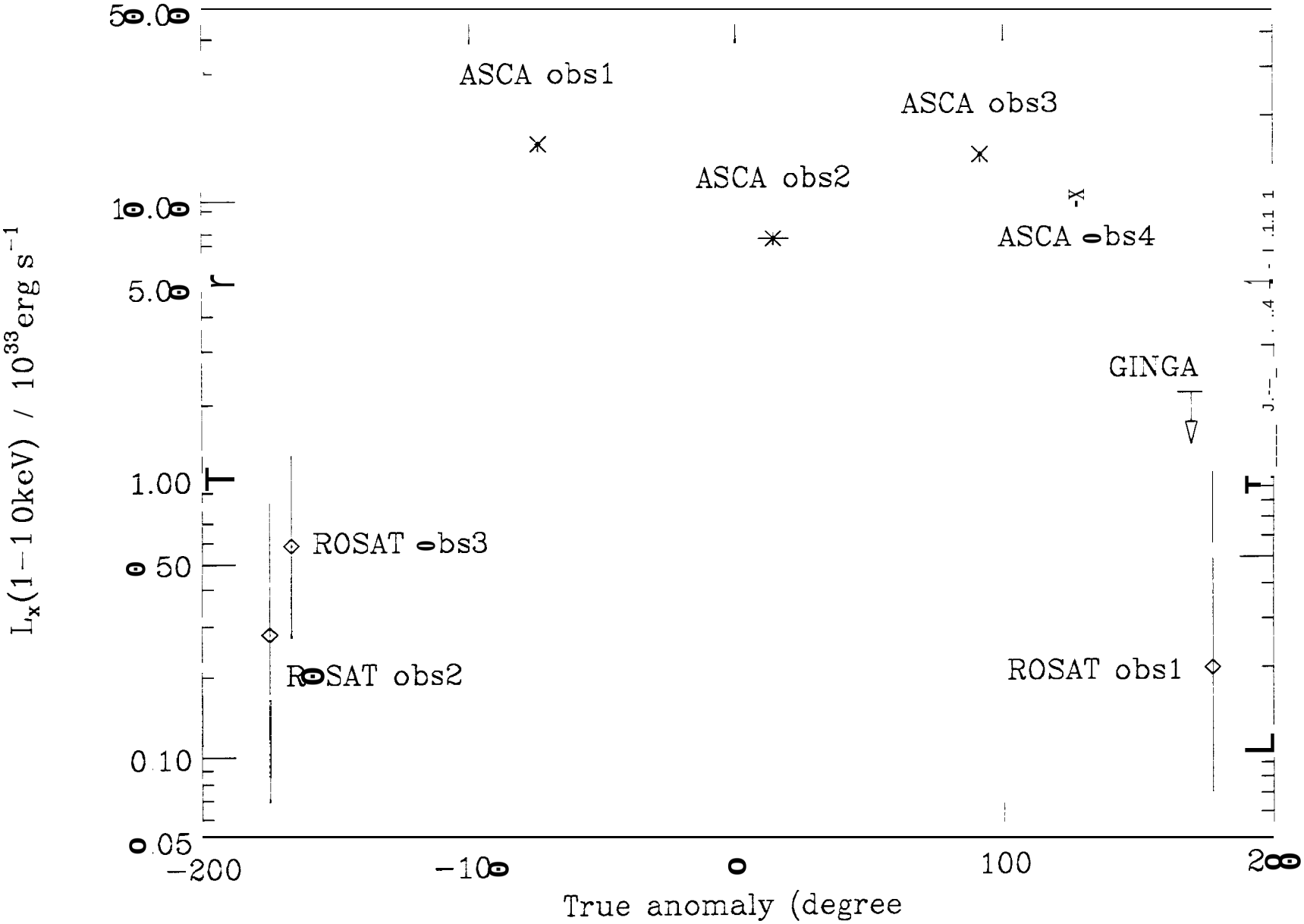
ASCA obs1
ASCA obs3
ASCA obs2
ASCA obs4
GINGA
ROSAT obs3
ROSAT obs2
ROSAT obs1
$L_x(1-10keV)$ / 10^{33}erg s^{-1}
True anomaly (degree